Journal of Molecular Catalysis A: Chemical 310 (2009) 34–41

Contents lists available at ScienceDirect

Journal of Molecular Catalysis A: Chemical

journal homepage: www.elsevier.com/locate/molcata

Catechol oxidase activity of dinuclear copper(II) complexes of Robson type macrocyclic ligands: Syntheses, X-ray crystal structure, spectroscopic characterization of the adducts and kinetic studies

Kazi Sabnam Banu[a], Tanmay Chattopadhyay[a], Arpita Banerjee[a], Santanu Bhattacharya[b], Ennio Zangrando[c,*], Debasis Das[a,*]

[a] Department of Chemistry, University of Calcutta, 92, A. P. C. Road, Kolkata-700 009, India
[b] Department of Chemistry, Maharaja Manindra Chandra College, Kolkata-700 003, India
[c] Dipartimento di Scienze Chimiche, University of Trieste, Via L. Giorgieri 1, 34127 Trieste, Italy

ARTICLE INFO

Article history:
Received 20 February 2009
Received in revised form 18 May 2009
Accepted 20 May 2009
Available online 27 May 2009

Keywords:
Catecholase activity
Copper(II)
Macrocyclic complexes
Schiff-bases
Template synthesis

ABSTRACT

Five dinuclear copper(II) complexes, $[Cu_2L^1(N_3)_2{\cdot}2H_2O]$ (**1**), $[Cu_2L^2(N_3)_2{\cdot}2H_2O]$ (**2**), $[Cu_2L^3(N_3)_2{\cdot}2H_2O]$ (**3**), $[Cu_2L^4(N_3)_2{\cdot}2H_2O]$ (**4**) and $[Cu_2L^5(N_3)_2{\cdot}2H_2O]$ (**5**) of Robson type macrocyclic Schiff-base ligands derived from [2+2] condensation of 4-methyl-2,6-diformylphenol with 1,3-diaminopropane (H_2L^1), 1,2-diaminoethane (H_2L^2), 1,2-diaminopropane (H_2L^3), 1,2-diamino-2-methylpropane (H_2L^4) and 1,2-diaminocyclohexane (H_2L^5), respectively have been synthesized and characterized. Catecholase activity of those complexes using 3,5-di-*tert*-butylcatechol as substrate has been investigated in two solvents, methanol and acetonitrile. The role of the solvent and of the steric properties of the macrocyclic ligand of these complexes on their catecholase activity has been examined thoroughly. Acetonitrile is observed to be a better solvent than methanol as far as their catalytic activity is concerned. However, methanol reveals to be a better choice to identify the enzyme–substrate adduct. The investigation also prompted that chelate ring size does affect on the catalytic efficiency: 6-membered ring (as in H_2L^1) exhibits better activity than its 5-membered counterpart (as in H_2L^2). The activity of the 5-membered counter parts also depend upon the steric factor. Moreover, the catalytic activity of the complexes is enhanced to a significant extent by increasing the bulkiness of the substituents on the backbone of macrocyclic H_2L^2 ligands.

1. Introduction

It is now well documented that copper containing metalloproteins play very important role in transport, activation and metabolism of dioxygen in living organism [1]. On the basis of spectroscopic evidences three types of active site were detected in copper proteins. However, a current classification distinguishes seven different types of active site in the oxidized state of copper containing proteins on the basis of recent developments achieved through spectroscopic and crystallographic techniques [2]. Catechol oxidase enzymes, usually observed in plant tissues and in some insects and crustaceans to catalyze the oxidation of catechols to the corresponding *o*-quinones (catecholase activity) are type-3 copper active site proteins [3]. The *o*-quinones are highly active compounds which readily undergo auto-polymerization with the formation of a brown polyphenolic pigment i.e. melanin, a route to protect tissue from damages by pathogens or insects [4]. A form of Catechol oxidase was first isolated in 1937 [5]. In 1998, Krebs and his co-workers determined the first crystal structure of the enzyme isolated from *Ipomoea batatas* (sweet potato) in three different states: the native *met* ($Cu^{II}Cu^{II}$) state, the reduced *deoxy* ($Cu^{I}Cu^{I}$) form and the complex with the phenylthiourea inhibitor [6]. In the native *met* state the two copper ions are separated by 2.9 Å and each metal center is coordinated by three histidine residues and bridged by a hydroxyl group. The coordination environment around each copper center can be best described as trigonal pyramid. In *deoxy* form, the two copper ions in their +1 oxidation state are at a considerably longer distance of 4.4 Å and the coordination environment around the two copper ions is distorted trigonal pyramid and square planar with one missing coordination site for the latter. The X-ray structural determination of Catechol oxidase from sweet potatoes *I. batatas* (*IbCO*) in different forms, gives us an ample opportunity to investigate the structure-function relationship and to get deep insight about the functional mechanism for developing ultimately accurate structural functional models of the native enzymes. In spite of tremendous efforts, the mecha-

* Corresponding author. Tel.: +91 33 2483 7031; fax: +91 33 2351 9755.
E-mail address: dasdebasis2001@yahoo.com (D. Das).

1381-1169/$ – see front matter © 2009 Elsevier B.V. All rights reserved.
doi:10.1016/j.molcata.2009.05.016

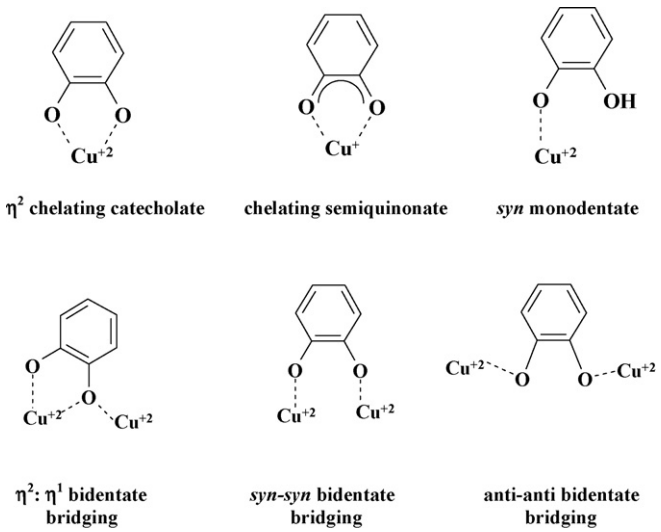

Scheme 1. Different possible binding modes of catechol to copper center(s).

nism even for the very first step is still a matter of debate [7–9] and Scheme 1 shows the various possible binding modes of catechol substrates to copper centers. The problem related to the binding mode of catechol to the copper centers makes it difficult to accept unanimously a satisfactory mechanism. At present only two mechanisms, based on biochemical, spectroscopic and structural data are widely accepted, one proposed by Krebs and co-workers [7] and the other by Solomon et al. [8]. The first step of the catalytic cycle involving a monodentate asymmetric coordination of the catechol to one copper center was proposed by Krebs et al. whereas simultaneous coordination of the substrate in the bidentate bridging mode to both the metal ions was the proposal of Solomon. The subsequent parts of the two mechanisms do not differ appreciably. Recently, Siegbahn [9] has suggested a radical mechanism on the basis of DFT calculation. According to him the active site of an enzyme like catechol oxidase which is deeply buried in the low dielectric of a protein, should not change its charge during the catalytic cycle and the catalytic cycle should starts from *deoxy*dicopper(I) form. However, at present no experimental finding is available to give support to the Siegbahn hypothesis. Our recent investigation [10] with dicopper(II) complexes of macroacyclic compartmental ligands enable us to establish that oxidation of catechol (3,5-DTBC) catalyzed by those complexes proceeds via the formation of two enzyme–substrate adducts. Thus, the first step of the catalytic cycle may be a combination of Kreb's and Solmon's proposals. Now we are interested to investigate catecholase activity of macrocyclic compartmental dicopper(II) complexes. For this purpose we have judiciously chosen a series of compartmental ligands H_2L^1–H_2L^5 (Scheme 2), popularly known as Robson's macrocycle [11], where the Cu–Cu separation may be kept about 3.0 Å. A literature survey suggests that such an intermetallic distance is one of the main criteria to exhibit efficient catechol oxidase activity. It is noteworthy that dicopper(II) complexes of "Robson" type macrocycle have previously been thoroughly investigated by several groups [12–18] especially to study the magneto-structural correlations and electrochemical properties. However, to the best of our knowledge, studies of catecholase activity of such system have not been reported till date.

We report herein the syntheses, characterization and catecholase activity of five dinuclear copper(II) complexes, $[Cu_2L^1(N_3)_2{\cdot}2H_2O]$ (**1**), $[Cu_2L^2(N_3)_2{\cdot}2H_2O]$ (**2**), $[Cu_2L^3(N_3)_2{\cdot}2H_2O]$

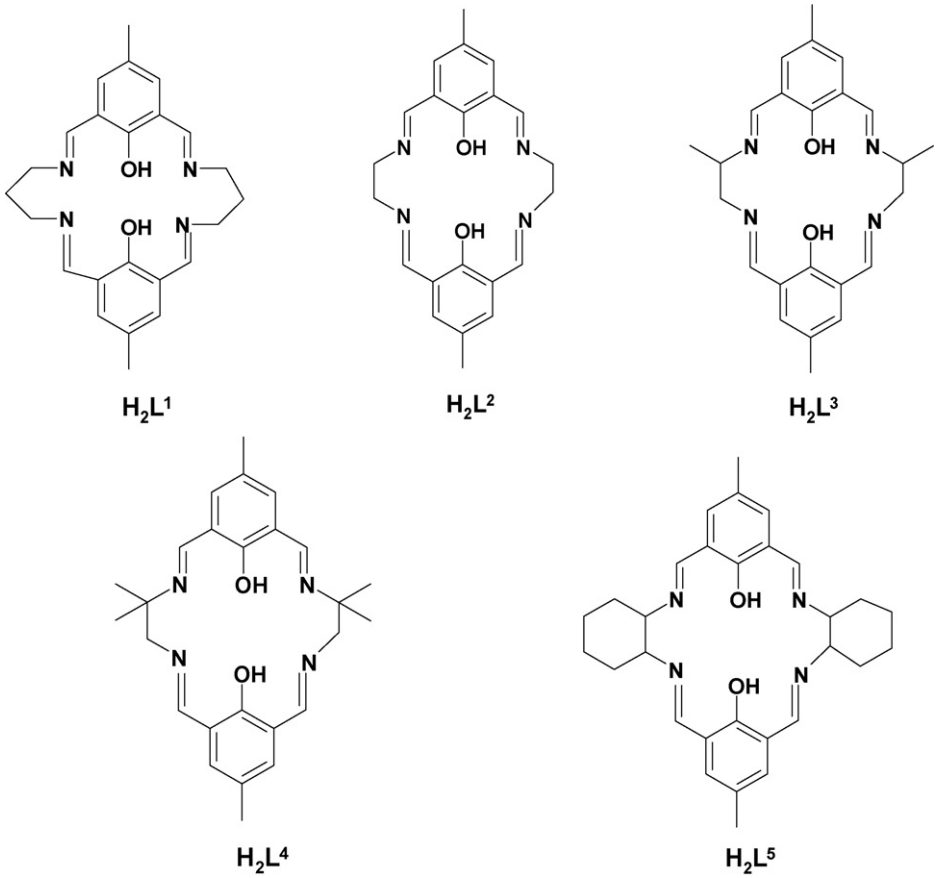

Scheme 2. Schematic representation of the macrocyclic ligand systems used in the present work.

Table 1
Electronic and infrared spectral data.

Compound	λ_{max} (nm) (ε, M^{-1} cm^{-1})			IR (KBr) (cm^{-1})
	In CH_3CN	In CH_3OH	In nujol	
1	354.33 (9764.18), 614.00 (53.03)	358.79 (1933.59), 611.32 (97.72)	350, 572	1633, 1562, 2019, 3442
2	375.00 (3691.25), 612.00 (210)	363.37 (8320.09), 598.62 (199.20)	360, 597	1622, 1540, 2027, 3424.2
3	369.64 (5005.67), 567.10 (140.72)	360.94 (8366.62), 537.31 (76.78)	365, 534	1623, 1548, 2035, 3424
4	374.81 (2062.35), 570.14 (77.72)	375.40 (2100.17), 568.32 (76.61)	370, 535	1623.9, 1541, 2035, 3448
5	372.24 (1879.9) 586.41 (41.11)	372.24 (1899.82), 587.78 (41.11)	374, 602	1629, 1546, 2037, 3469

(**3**), $[Cu_2L^4(N_3)_2{\cdot}2H_2O]$ (**4**) and $[Cu_2L^5(N_3)_2{\cdot}2H_2O]$ (**5**) of compartmental Schiff-base ligands derived from 2 + 2 condensation of 4-methyl-2,6-diformylphenol with 1,3-diaminopropane, 1,2-diaminoethane, 1,2-diaminopropane, 2-methyl-1,2-diaminopropane and 1,2-diaminocyclohexane, respectively. Our investigation ascertains the role of solvent and of the steric properties of the macrocyclic ligand attached to the copper centre on their catechol oxidase activity.

2. Results and discussion

2.1. Syntheses procedure and characterizations

Complexes **1**–**5** were synthesized by applying template synthesis technique by treating methanolic solution of copper(II) nitrate trihydrate with the Schiff-bases which were formed in situ by the condensation of 4-methyl-2,6-diformylphenol and the corresponding diamines (1,3-diaminopropane, 1,2-diaminoethane, 1,2-diaminopropane, 2-methyl-1,2-diamino-propane and 1,2-diaminocyclohexane) in the presence of excess sodium azide in the ratio 1.15: 1:1.3: 4.3 as reported earlier [18]. The IR and UV–vis spectral data for complexes **1**–**5** are given in Table 1. All the complexes exhibit C═N stretching frequencies in the range of 1623–1633 cm^{-1} and skeletal vibration at 1540–1560 cm^{-1} indicating that there is no free NH_2 or C═O bond present in the ligand systems of complexes **1**–**5**. Therefore all the complexes are macrocyclic in nature. There is no broad band centered at around 1380 cm^{-1} indicating the absence of NO_3^-, while in all cases a very strong single sharp band is obtained at the range of 2019–2036 cm^{-1} characteristic of symmetrically bonded azido ligand. However, from IR spectra alone it is very difficult to assign the coordination mode of the azido ligand. All the complexes show bands at around 3290–3430 cm^{-1} suggesting the presence of water molecules in them. The thermogravimetric analysis suggests the presence of two molecules of water per molecule of the complexes (vide Section 3). The electronic spectra of complexes **1**–**5** have been studied in the solid-state (dispersed in nujol mull) as well as in solution using acetonitrile and methanol as solvent. The absorption band observed in the range of 560–620 nm corresponds to d–d transition and the strong bands at 350–400 nm are due to the phenoxo-Cu^{II} LMCT. In **1**–**5**, the positions of d–d transition bands are in agreement with a square-pyramidal geometry around the metal centers [19]. Since no significant shifting in band positions is observed in solid-state electronic spectra of **1**–**5** (Table 1) in compare to the corresponding spectra recorded in solution, it may be assumed that solution and solid-state structures of the complexes are very much similar. The structural characterization of complex **2** has already been reported by us [18] while efforts to synthesize single crystals of remaining complexes have got success in case of complex **1** only. However, in order to get the structural composition of these species in solution, we performed ESI-MS study of complexes **3**, **4** and **5**. In methanol, the most abundant peak(s) (base peak) is observed at 693.32 for **3** (calculated *m*/*z*: 693.63 amu); 648.85 (calculated *m*/*z*: 649.62 amu) for **4** and 719.77 for **5** (calculated *m*/*z*: 719.71 amu). These results corroborate well with the respective monopositive species of formulation $[C_{25}H_{40}O_8N_4Cu_2]^+$, $[C_{27}H_{36}O_4N_7Cu_2]^+$, and $[C_{31}H_{42}O_5N_7Cu_2]^+$ for complex **3**, **4** and **5**, respectively (SI file).

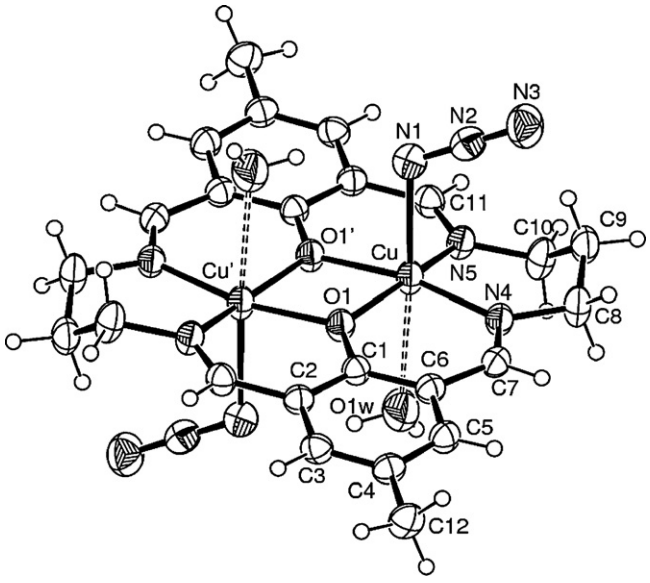

Fig. 1. ORTEP drawing (40% probability ellipsoid) of the dinuclear complex **I** located on a symmetry center with labelling scheme of independent atoms.

2.1.1. Description of structure of complex *1*

An ORTEP view of the complex **1** with atom labeling scheme of the independent part is shown in Fig. 1 and inter atomic distances and angles relevant to the copper coordination sphere are given in Table 2. The macrocyclic ligand is basically flat, except for the methylene carbon atoms C (9) and C (10) of propylene bridge. The symmetry related metal ions present a square planar pyramidal geometry, being bonded by two imine nitrogen atoms, two bridging phenolate oxygens and an azide anion. It seems more appropriate to indicate the coordination geometry as indicated rather than octahedral since the water molecule O1w (Fig. 1), which occupies the

Table 2
Selected bond distances (Å) and angles (°) with their estimated standard deviations for complex **1**.

Cu–N(4)	1.9845(17)	Cu–O(1)	1.9770(14)
Cu–N(5)	1.9692(17)	Cu–O(1′)	1.9867(14)
		Cu–N(1)	2.373(2)
N(4)–Cu–N(5)	97.05(7)	N(5)–Cu–N(1)	96.96(8)
N(4)–Cu–O(1)	93.04(6)	O(1)–Cu–O(1′)	76.93(6)
N(4)–Cu–O(1′)	168.06(6)	O(1)–Cu–N(1)	93.53(7)
N(4)–Cu–N(1)	96.30(7)	O(1′)–Cu–N(1)	90.82(7)
N(5)–Cu–O(1)	164.54(6)	N(2)–N(1)–Cu	115.54(16)
N(5)–Cu–O(1′)	91.56(6)	N(3)–N(2)–N(1)	178.8(3)

Primed atoms at $-x+1,-y+1,-z+1$.

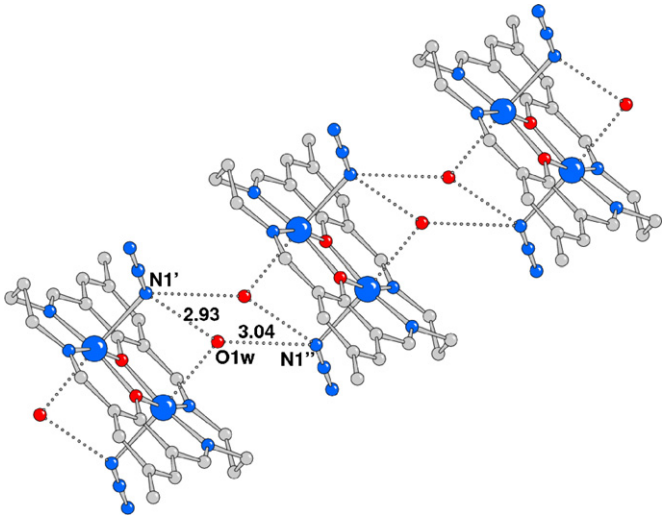

Fig. 2. Packing arrangement with indication of the H-bonding distances occurring between the water molecule (at half occupancy) and azide nitrogen. N (1′) at $1-x$, $1-y$, $1-z$; N(1″) at x, y, $1+z$.

other axial position at much longer distance, 2.689(4) Å, presents a half occupancy. The Cu–O and Cu–N bonds are comparable in length varying from 1.969(2) Å average to 1.987(1) Å, while the apical Cu–N (azide) is significantly longer of 2.373(2) Å. The copper ion is slightly displaced from the strictly planar N_2O_2 donor set toward the azide nitrogen donor by 0.158(1) Å. The bond angle Cu–O(1)–Cu′ of 103.07(6) Å leads to an inter metallic separation of 3.099(2) Å, which is close comparable to the values measured in complexes containing the same macromolecular system with different counter ions [11–18]. The crystallographic investigation reveals 1D polymeric chains (Fig. 2), developed along axis *b*, based on weak hydrogen-bond interactions occurring between the water molecules and the azide groups of symmetry related complexes. A survey of the literature of these systems indicates that the crystal packing is strongly dictated by the counter ion nature and the present complex represents another example of polymeric structure, beside the arrangements built up by $Co(CN)_6^{4-}$ and $Cr(oxalate)_3^{3-}$ anions, [12(c)] and by ethyne-1,2-dicarboxylato [17]. The intermetallic distance found in **1**, of 3.099(2) Å, is well within the range measured in similar crystal structure derivatives (20 values, 3.034–3.233 Å). On the other hand, this distance is significantly longer than the values observed for complexes with an ethyl bridge (L^2) 2.792–2.962 Å, and also with respect to the distance found in two structures having a hexyl bridge (like L^5) of 2.872 and 2.889 Å [14].

2.2. UV–vis spectrophotometric study for catechol oxidase activity of the complexes using 3,5-di-tert-butylcatechol as substrate

3,5-di-*tert*-butylcatechol (3,5-DTBC) is the most widely used substrate for the study of catecholase activity mainly because of the following reasons: (i) it is easy to oxidize due to low quinone–catechol reduction potential; (ii) the oxidized species, 3,5-DTBQ is stable for at least 6 h and (iii) 3,5-DTBQ has characteristic absorption band maxima at 403 and 401 nm in acetonitrile and methanol, respectively, the two largely used solvents to study the catecholase activity. Before proceeding into the detailed kinetic study, we need to check the ability of our Cu^{II} complexes to catalyze the oxidation of 3,5-DTBC. For this purpose, 1×10^{-4} mol dm^{-3} solutions (in methanol as well as acetonitrile) of complexes **1**–**5** were treated with 1×10^{-2} mol dm^{-3} (100 equivalents) of 3,5-DTBC at 25 °C under aerobic condition.

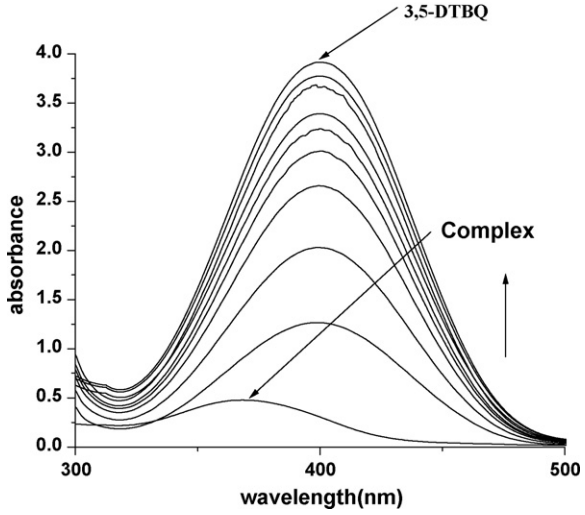

Fig. 3. The variation of the spectral behavior of complex **3** (as representative of complexes **3**–**5**) in followed up for two hrs in acetonitrile solution.

2.2.1. UV–vis spectral study in acetonitrile

The complexes **1**, **3**, **4** and **5** behave similarly with 3,5-DTBC as is evident from their time dependent spectral scan in acetonitrile medium. Fig. 3 represents the variation of the spectral behavior of complex **3** as a representative (other spectral data are in SI file) in presence of 3,5-DTBC. The figure clearly shows that the complex catalyzes the oxidation of 3,5-DTBC to 3,5-DTBQ smoothly. On the other hand, complex **2** (Fig. 4) behaves differently with 3,5-DTBC. Even after two hrs. course of reaction, no band centered at around 400 nm is observed though an enhancement of absorbance on the parents band maxima are noticed which is probably due to the formation of an adduct between Cu^{II} and 3,5-DTBC.

2.2.2. UV–vis spectral study in methanol

Complex **1** and **5** are observed to catalyze the oxidation of 3,5-DTBC to 3,5-DTBQ in methanol. Fig. 5 shows the change of spectral behavior of complex **1** (representative of the two) on reaction with 3,5-DTBC upto 2 h course of reaction. On the other hand, the complexes **2**–**4** are found to be inactive in methanol medium to catalyze the oxidation although all of them generate stable adducts with the substrate as is evident from their time dependent spectral scan (Fig. 6 for complex **2** as a representative).

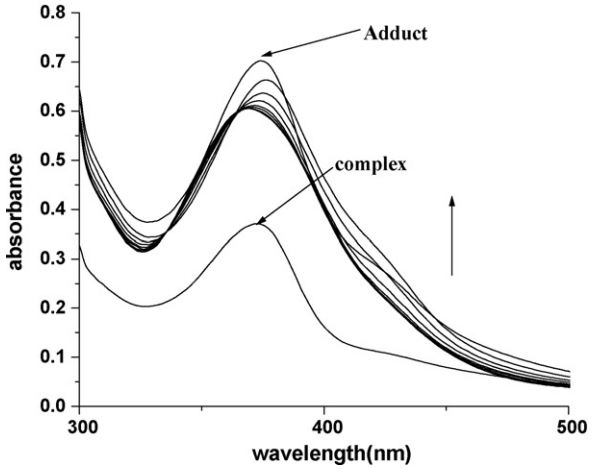

Fig. 4. The variation of the spectral behavior after addition of 3,5-DTBC (1:100) to acetonitrile solution of complex **2** followed up for 2 h.

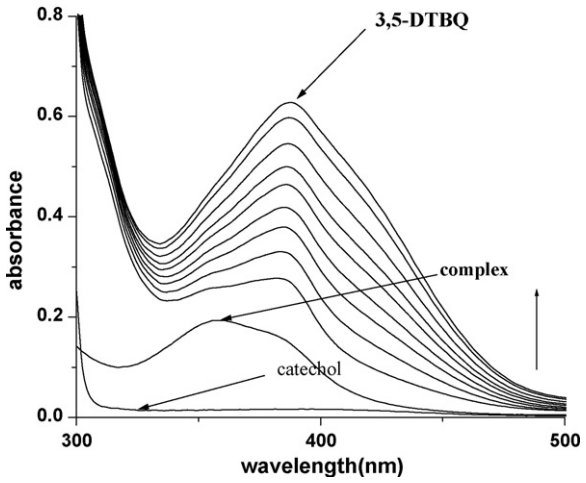

Fig. 5. The spectral scan of the methanolic solution of complex **1** (representative of complexes **1** and **5**) after the addition of 3,5-DTBC followed up for 2 h.

2.2.3. Characterization of the complex–substrate adduct by ESI-MS study

From the time dependent spectral scan as discussed above it is evident that complex **2** in acetonitrile and complexes **2**, **3** and **4** in methanol medium form stable adduct with 3,5-DTBC. Our all attempts to obtain single crystals of those complex–substrate adducts were unsuccessful. We then tried to characterize the species with the help of ESI-MS study. For this purpose we have chosen complex **3** to perform the experiment. Complex **3** in methanol exhibits base peak at 693.32, corresponding to the monopositive species **3a** (calculated *m*/*z*: 693.63 amu) (Scheme 3). The ESI-MS spectrum taken immediately after the addition of 3,5-DTBC (maintaining complex: 3,5-DTBC as 1:100) shows the major peaks at 463.04 (calculated *m*/*z*: 465.07 amu) and 294.28 amu (calculated *m*/*z*: 293.69) which corroborate well with the di- and tri-positive species, **3b** and **3c**, respectively (Scheme 3). However, it is to note that isotopic distribution patterns of these species do not agree with di- and tri-positive nature, but rather to monopositive charged species. Thus, it is difficult to come to a definite conclusion regarding the structure of the complex–substrate adduct based on ESI-MS study only and for this, further extensive work is necessary which is underway in our laboratory. In our previous communication [10] we have established that oxidation of 3,5-DTBC to 3,5-DTBQ by molecular oxygen proceeds via the formation of two enzyme–substrate adducts, ES1 and ES2. The adduct ES1 justifies the proposal of Krebs and his co-workers (catechol coordination to copper center in a monodentate fashion), whereas ES2 supports the mechanism advocated by Solomon and his group (bidentate coordination mode of catechol to the copper centers). In our present set of complexes monodentate catechol coordination is more likely over the bidentate fashion due to the presence of strongly bonded azido ligands, in *trans* position with respect to the mean plane of the complex. Our ESI-MS study is also in well agreement with this proposition.

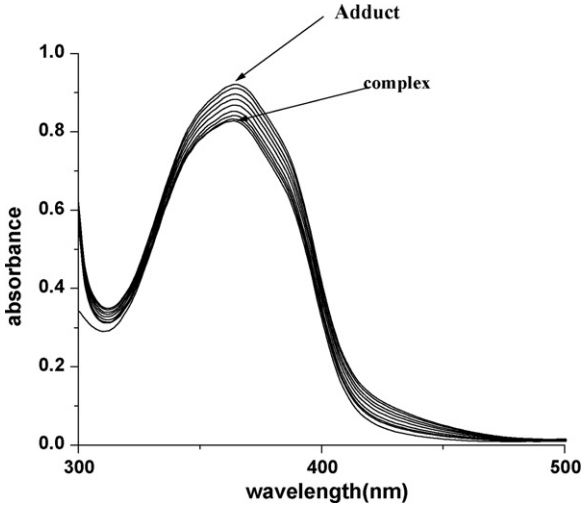

Fig. 6. The spectral scan of the methanolic solution of **2** (representative of complexes **2**–**4**) after the addition of 3,5-DTBC followed up for two hrs.

2.3. Catechol oxidase activity and kinetic study

The kinetics of the formation of 3,5-DTBQ catalyzed by complexes **1** and **5** were performed in methanol as well as in acetonitrile in order to get better understanding of the solvent effect. For complexes **3** and **4** the same has been conducted in acetonitrile medium only. In all the cases the experimental procedure involves the monitoring of the increase in concentration of the product, 3,5-DTBQ with time. The concentration of the substrate 3,5-DTBC was always kept at least 10 times larger than that of Cu^{II} complex to maintain pseudo first order condition. All the kinetic experiments were conducted at constant temperature of 25 °C by using a thermostat. Solutions containing different concentrations of substrate 3,5-DTBC were prepared (1×10^{-3} mol dm^{-3} to 1×10^{-2} mol dm^{-3}) from a concentrated stock solution. 2 mL of this substrate solution (in methanol or in acetonitrile) was taken in a 1 cm quartz cell which was kept inside the spectrophotometer cell holder for a while to attain the temperature (25 °C). Then 0.04 ml (2 drops) of 5×10^{-3} mol dm^{-3} of Cu^{II} macrocyclic complex in methanol/acetonitrile medium was quickly added and mixed properly so that the ultimate concentration of Cu^{II} complex becomes 1×10^{-4} mol dm^{-3}. The time scan was started as quickly as possible and the absorbance variation with time was continuously monitored at 400 nm. Initial rate method is applied to evaluate the rate constant for the formation of 3,5-DTBQ. At least three runs were taken for each concentration and the initial rates are determined from the slope of the tangent to the absorbance vs time curve at $t = 0$. Fig. 7 represents the dependence of initial rate on the concentration of catechol for complex **5** (as representative, the data for other complexes are in SI file). By applying *GraFit32* pro-

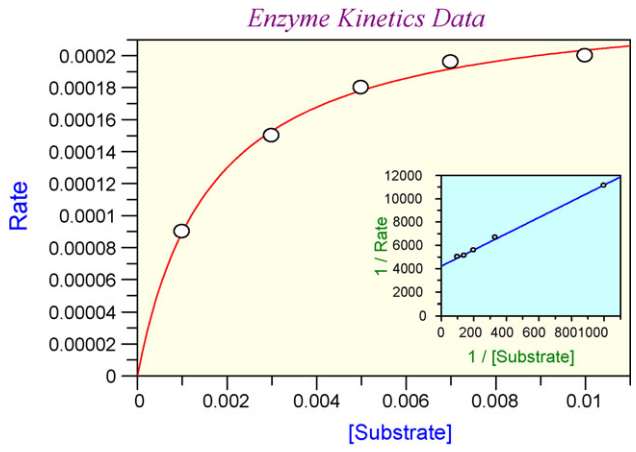

Parameter	Value	Std. Error
Vmax	0.0002	5.32546e-006
Km	0.0017	0.0001

Fig. 7. Plot of rate vs concentration of **5**. Plot of inset shows reciprocal Lineweaver–Burk plot for the same complex.

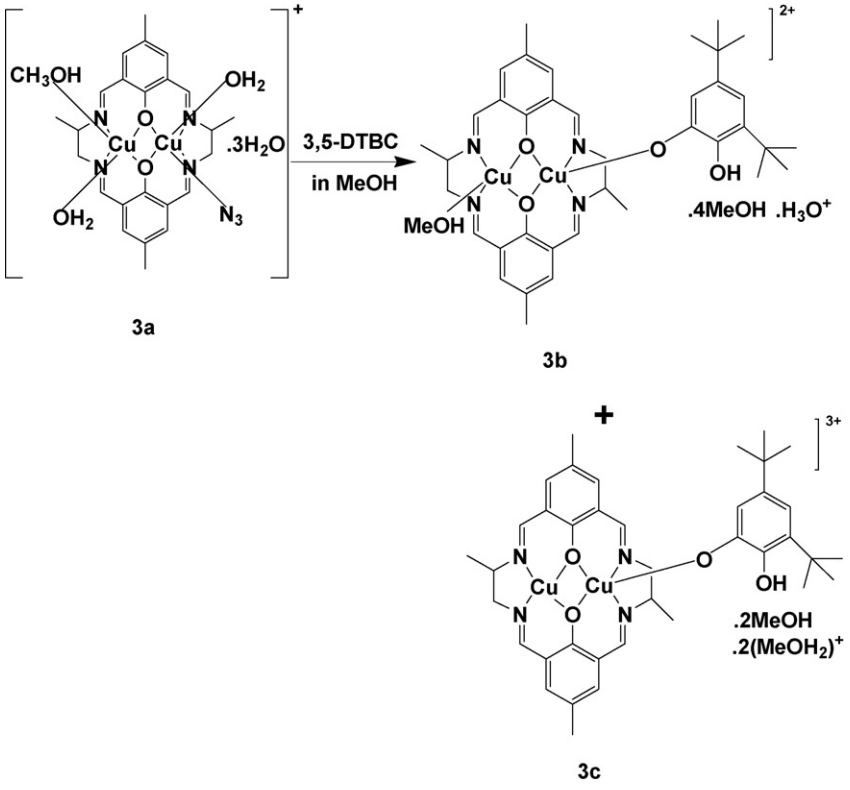

Scheme 3. Probable structure of complex **3** in methanol (**3a**) and complex 3,5-DTBC adducts (**3b** and **3c**) according to ESI-MS study.

gramme for enzymatic kinetics, Michaelis–Menten constant (K_M) and maximum velocity (V_{max}) can be calculated and the inset shows the Lineweaver–Burk plot. Furthermore, a linear relationship for the initial rate was obtained for a particular concentration of the substrate and varying the concentration of Cu^{II} complex which suggests the first order dependence of rate on the concentration of Cu^{II} complex. Now keeping the concentration of Cu^{II} complex fixed and varying the 3,5-DTBC concentration, a first order dependence was observed at low concentration of 3,5-DTBC. However, all the Cu^{II} macrocyclic complexes showed a saturation kinetic at higher concentration of 3,5-DTBC. Thus a treatment on the basis of Michaelis–Menten model was seemed to be appropriate. Fig. 8 shows the Lineweaver–Burk plots (double reciprocal plot) for the complexes. From these plots parameters such as V_{max}, rate constant for the dissociation of complex–substrate intermediate (i.e. the turnover number, k_{cat}) and K_M were evaluated for the different complexes and the data tabulated in Table 3. Although the mechanism of the reaction appears to be complicated at first sight, the data obtained from Lineweaver–Burk plot are adequate for an assessment of the catalytic activity. The present complexes demonstrate to be excellent catalyst for conversion of 3,5-DTBC to 3,5-DTBQ. The observed k_{cat} ranges from $7.20 \times 10^3\ h^{-1}$ to $2.16 \times 10^4\ h^{-1}$ and the higher value may be compared with that of $3.2 \times 10^4\ h^{-1}$ of the most efficient catalyst reported till date exhibited by a macroacyclic dinuclear copper(II) complex [10].

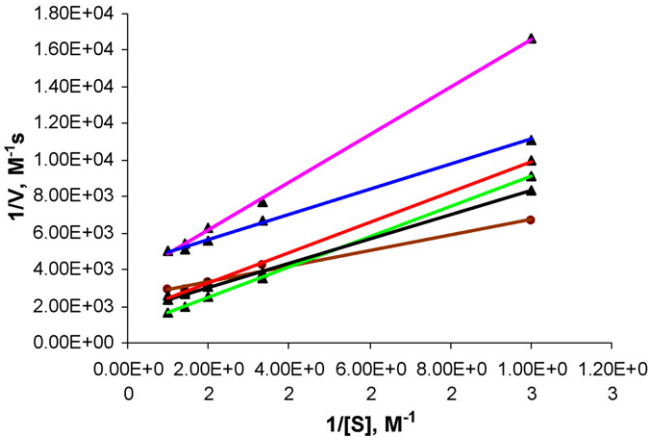

Fig. 8. Lineweaver–Burk plots (double reciprocal plot) for the complexes: ( ) for **1** in methanol, ( ) for **1** in acetonitrile, ( ) for **3** in acetonitrile, ( ) for **4** in acetonitrile, ( ) and ( ) for **5** in acetonitrile and methanol respectively.

2.4. Solvent effect

From the above UV–vis spectral study it appears that there is a strong solvent effect on the catalytic efficiency of the complexes

Table 3
Kinetic parameters for complexes **1, 3, 4** and **5**.

Complex	Solvent	V_{max} ($M\,s^{-1}$)	K_M (M)	k_{cat} (h^{-1})
1	Methanol	$(5.00 \pm 0.06) \times 10^{-4}$	$(23.0 \pm 1.00) \times 10^{-4}$	$(1.80 \pm 0.02) \times 10^4$
1	Acetonitrile	$(6.00 \pm 0.10) \times 10^{-4}$	$(9.70 \pm 0.30) \times 10^{-3}$	$(2.16 \pm 0.03) \times 10^4$
3	Acetonitrile	$(3.00 \pm 0.09) \times 10^{-4}$	$(3.80 \pm 0.30) \times 10^{-3}$	$(1.08 \pm 0.03) \times 10^4$
4	Acetonitrile	$(5.00 \pm 0.38) \times 10^{-4}$	$(3.40 \pm 0.70) \times 10^{-3}$	$(1.80 \pm 0.13) \times 10^4$
5	Acetonitrile	$(6.00 \pm 0.10) \times 10^{-4}$	$(3.70 \pm 0.20) \times 10^{-3}$	$(2.16 \pm 0.03) \times 10^4$
5	Methanol	$(2.00 \pm 0.05) \times 10^{-4}$	$(1.70 \pm 0.01) \times 10^{-3}$	$(7.20 \pm 0.18) \times 10^3$

to catalyze the oxidation of 3,5-DTBC to 3,5-DTBQ. Acetonitrile appears to be a better solvent than methanol as far as the catalytic activity is concerned. The k_{cat} values (Table 3) for complex **1** and **5** in methanol as well as in acetonitrile medium are in excellent agreement with the above fact. This may be related to the difference in polarity and ability to form the hydrogen bonding of the two solvents. However, methanol reveals to be a better choice to identify the enzyme–substrate adduct because of the fact that the adduct attains greater stability in methanol in comparison to acetonitrile.

2.5. Effect of Ligand backbone

Complex **1**, in which the macrocyclic ligand (H_2L^1) is the 2 + 2 condensation product of 2,6-diformyl-4-methylphenol and 1,3-diaminopropane, is observed to be equally efficient as catalyst in both the solvents, whereas complex **2** made of with the macrocyclic ligand H_2L^2, a [2 + 2] condensation product of 4-methyl-2,6-diformylphenol and 1,2-diaminoethane is found to be inactive in both the solvents to catalyze the oxidation of 3,5-DTBC under our experimental condition. These data suggest that size of the chelate ring does affect on the catalytic efficiency: 6-memberd ring (as in H_2L^1) exhibits better activity than its 5-membered counterpart (as in H_2L^2). The analysis of crystal structures reveal that the ligand L^1 induces a slightly larger intermetallic distance [3.099(2) Å] with respect to the complexes containing L^2–L^5 (2.792–2.962 Å), a feature that could influence the catalytic process. Moreover, it is to note that the catalytic activity of the complexes may be modified to a significant extent by changing the steric and electronic factors on the backbone of macrocyclic H_2L^2 by changing the alkyl substituents.

The oxidation of 3,5-DTBC to 3,5-DTBQ is a two electrons oxidation process. In our complexes each copper ion is in +2 oxidation state and it may undergo reduction to Cu^I state in the catalytic cycle during the oxidation of 3,5-DTBC to 3,5-DTBQ. On changing the substituents on the backbone of the macrocyclic ligand from methyl- to 1,1-dimethyl- and to cyclohexyl-, the +I effect increases gradually which reduces the positive charge density on Cu^{II} centre and thereby reduces the possibility to undergo reduction of Cu^{II} centre to Cu^I. Consequently a decrease of catalytic activity of the corresponding complexes should be expected from complex **2**–**5**. But contrary to this, a gradual increment of the efficiency is observed on going from **2**–**5**. Then we address our attention to the possible role exerted by alkyl group (between the N atoms), having different steric demand from L^1 to L^5. Taking into account that all the complexes in solution have the same coordination environment (same axial ligand/s), the Cu^{II} center appears more accessible towards the substrate in case of complex **1** (more flexible 6-membered chelate ring formed by the imine part of ligand L^1 and at the same time more steric crowding exerted in compare to ligand L^2) and complex **5** (having ligand which is the most sterically crowded derivative of L^2). From structural point of view the two copper centers exhibit maximum non co-planarity in complex **1** and **5**. In other words the accessibility of one copper center to bind with the substrate 3,5-DTBC is observed to attend the maximum in complex **1** and **5** and consequently they exhibit the highest catecholase activity (in terms of k_{cat} value, Table 3).

3. Experimental

3.1. Starting materials

All materials were obtained from commercial sources and used as purchased. Solvents were dried according to standard procedure and distilled prior to use. 4-methyl-2,6-diformylphenol was prepared according to the literature method [13]. 1,3-diaminopropane, 1,2-diaminoethane, 1,2-diaminopropane, 1,2-diamino-2-methylpropane, 1,2-diaminocyclohexane were purchased from Aldrich Chemical Company Inc. and used as received. All other chemicals used here were of AR grade.

3.2. Physical measurements

Elemental analyses (carbon, hydrogen and nitrogen) were performed using a PerkinElmer 240C elemental analyzer. Copper was estimated gravimetrically with α-benzoin oxime. Infrared spectra (4000–400 cm^{-1}) were recorded at 27 °C using a Shimadzu FTIR-8400S where KBr was used as medium. Electronic spectra (800–200 nm) were obtained at 27 °C using a Shimadzu UV-3101PC where dry acetonitrile/dry methanol/nujol was used as a medium as well as reference. The electrospray mass spectra were recorded on a MICROMASS Q-TOF mass spectrometer. Thermal analyses (TG–DTA) were carried out on a Shimadzu DT-30 thermal analyzer in flowing dinitrogen (flow rate: 30 cm^3 min^{-1}).

3.3. Syntheses of the complexes

All the complexes were synthesized by following the same procedure as we reported earlier to prepare complex **2** [18]. Typically a methanolic solution (5 ml) of a diamine [1,3-diaminopropane/1,2-diaminoethane/1,2-diaminopropane/1,2-diamino-2-methylpropane/1,2-diaminocyclohexane] (2.3 mmol) was added to a clear solution of $Cu(NO_3)_2{\cdot}3H_2O$ (2.07 mmol) dissolved in 8 ml of methanol, which produced immediately an intensely blue solution. The solution was then refluxed and a 5 ml of methanolic solution of 4-methyl-2,6-diformylphenol (3.6 mmol) was added drop wise over 2 h in refluxing condition. After the completion of the addition of 4-methyl-2,6-diformylphenol, the reflux was continued for additional 30 min. On cooling the mixture reddish green slurry was formed. This slurry was filtered out and a deep green filtrate was obtained. An excess amount of sodium azide (7.7 mmol) dissolved in the minimum amount of water was then added to that deep green filtrate part, immediately a brown precipitate was formed. It was filtered and the deep green filtrate part was kept in a $CaCl_2$ desiccator in dark. After a few days, crystals of the complex suitable for X-ray data collection were separated out. The crystals were filtered out and washed with methanol and dried in air. The filtrate was kept again in a $CaCl_2$ desiccator in dark. The filtrate parts obtained after separation of complex **1** and **3**–**5** yield solid mass as mixture of products [20].

Caution. Azide salts are potentially explosive and should be handled with small quantities with care. No problems were faced with the complexes reported herein.

3.3.1. $[Cu_2L^1(N_3)_2{\cdot}2H_2O]$ (**1**)

Yield 63%. Anal. calcd. for $C_{24}H_{30}N_{10}O_4Cu_2$ (649.57): calcd. C, 44.37; H, 4.62; N, 21.57; Found: C, 44.35; H, 4.63; N, 21.55; TG analysis: 1.121 mg weight loss (5.605% of 20 mg complex, expected weight loss: 5.545%) at 130 °C.

3.3.2. $[Cu_2L^2(N_3)_2{\cdot}2H_2O]$ (**2**)

Yield 35%. Anal. calcd. for $C_{22}H_{26}N_{10}O_4Cu_2$ (621.51): calcd. C, 45.74; H, 4.76; N, 22.23; Found: C, 42.73; H, 4.80; N, 22.24; TG analysis: 1.164 mg weight loss (5.820% of 20 mg complex, expected weight loss: 5.790%) at 137 °C.

3.3.3. $[Cu_2L^3(N_3)_2{\cdot}2H_2O]$ (**3**)

Yield 69%. Anal. calcd. for $C_{24}H_{30}N_{10}O_4Cu_2$ (649.57): calcd. C, 44.37; H, 4.62; N, 21.57. Found: C, 44.35; H, 4.63; N, 21.55. TG analysis: 1.116 mg weight loss (5.580% of 20 mg complex, expected weight loss: 5.545%) at 143 °C.

Table 4
Crystallographic data and structure refinement details for complex **1**.

Empirical formula	$C_{24}H_{26}Cu_2N_{10}O_3$
Formula weight	629.63
T (K)	293
Mo-Kα	0.71073
Crystal system	monoclinic
Space group	$P2_1/c$
a (Å)	10.716(3)
b (Å)	15.926(3)
c (Å)	7.281(3)
β (○)	90.27
V (Å^3)	1242.6(7)
Z	2
D_{calc} (g/cm^3)	1.683
F (0 0 0)	644
μ (mm^{-1})	1.762
θ Range (°)	3.19–29.62
Reflection collected	15297
Independent reflection	3476
Reflection observed	2582
Goodness-of-fit on F^2	0.952
Rint	0.0459
Final R indices [$I > 2(I)$]	$R1 = 0.0341$, $wR2 = 0.0874$
Final R indices (all data)	$R1 = 0.0488$, $wR2 = 0.0926$

$w = 1/[\sigma^2(F_o^2) + (0.1759P)^2 + 22.5743P]$, where $P = (F_o^2 + 2F_2^c)/3$.

3.3.4. $[Cu_2L^4(N_3)_2{\cdot}2H_2O]$ (**4**)

Yield 67%. Anal. calcd. for $C_{26}H_{34}N_{10}O_4Cu_2$ (677.62): calcd. C, 46.08; H, 5.02; N, 20.67. Found: C, 44.11; H, 5.07; N, 2072. TG analysis: 1.076 mg weight loss (5.382% of 20 mg complex, expected weight loss: 5.317%) at 133 °C.

3.3.5. $[Cu_2L^5(N_3)_2{\cdot}2H_2O]$ (**5**)

Yield 72%. Anal. calcd. for $C_{30}H_{38}N_{10}O_4Cu_2$ (729.70): calcd. C, 49.38; H, 5.21; N, 19.20. Found: C, 49.40; H, 5.47; N, 19.24. TG analysis: 1.002 mg weight loss (5.012% of 20 mg complex, expected weight loss: 4.938%) at 135 °C.

3.4. X-ray Data Collection and crystal structure determinations

Diffraction data for **1** were collected at room temperature on a Nonius DIP-1030H system (Mo-Kα radiation, λ = 0.71073 Å). Cell refinement, indexing and scaling of the data set were carried out using packages Denzo and Scalepack [21]. The structure was solved by direct methods and subsequent Fourier analyses [22] and refined by the full-matrix least-squares method based on F^2 with all reflections. A disorder water molecule (0.5 factor occupancy), accounting for one molecule per complex unit was detected in the Fourier map. The H atoms at calculated position were included in the final cycles of refinement. All the calculations were performed using the WinGX System, Ver 1.70.01 [23]. Selected crystallographic data and refinement details are displayed in Table 4.

4. Conclusion

Five dinuclear copper(II) complexes of Robson type macrocyclic ligands have been synthesized and comprehensively characterized. Catecholase activity of these complexes has been investigated by using 3,5-DTBC as substrate in two different solvents, acetonitrile and methanol. Our study indicates that the alkyl bridge between the imine nitrogens of macrocyclic ligand does affect on the catalytic efficiency of the corresponding complexes. The complex in which the imine part of the macrocyclic ligand system is bearing 6-membered chelate ring is observed to be more efficient to catalyze the oxidation of 3,5-DTBC in presence of molecular oxygen than that having 5-membered chelate ring. Thus, complex **1** is observed to be the most efficient catalyst. However, the catalytic efficiency of 5-membered chelate ring complexes are observed to be largely influenced by the nature of the alkyl substituents present on the ligand backbone where the steric demands prevail over the electronic factor of the alkyl substituent and thus complex **5** shows the highest efficiency amongst the complexes of macrocyclic ligands of H_2L^2 and its derivatives (forming 5-membered chelate ring). The nature of the solvent plays an important role on the catalytic activity of the complexes as well and acetonitrile is found to be a better choice to study the catecholase activity of dinuclear copper(II) complexes of "Robson" type macrocyclic ligands presented here. As far as the binding mode of 3,5-DTBC is concerned monodentate mode of coordination seems to be more justified.

Appendix A. Supplementary data

Supplementary data associated with this article can be found, in the online version, at doi:10.1016/j.molcata.2009.05.016.

References

[1] R.H. Holm, P. Kennepohl, E.I. Solomon, Chem. Rev. 96 (1996) 2239.
[2] I.A. Koval, P. Gamez, C.K. Selmeczib, J. Reedijk, Chem. Soc. Rev. 35 (2006) 814.
[3] A. Rompel, H. Fischer, D. Meiwes, K. Bu¨ldt-Karentzopoulos, R. Dillinger, H. Tuczek, Witzel, B. Krebs, J. Biol. Inorg. Chem. 4 (1999) 56.
[4] B.J. Dervall, Nature 189 (1961) 311.
[5] A.M. Mayer, E. Harel, Phytochemistry 18 (1979) 193.
[6] (a) T. Klabunde, C. Eicken, J.C. Sacchettini, B. Krebs, Nat. Struct. Biol. 5 (1998) 1084;
(b) C. Gerdemann, C. Eicken, B. Krebs, Acc. Chem. Res. 35 (2002) 183.
[7] C. Eicken, B. Krebs, J.C. Sacchettini, Curr. Opin. Struct. Biol. 9 (1999) 677.
[8] E.I. Solomon, U.M. Sundaram, T.E. Machonkin, Chem. Rev. 96 (1996) 2563.
[9] P.E.M. Siegbahn, J. Biol. Inorg. Chem. 9 (2004) 577.
[10] K.S. Banu, T. Chattopadhyay, A. Banerjee, S. Bhattacharya, E. Suresh, M. Nethaji, E. Zangrando, D. Das, Inorg. Chem. 47 (2008) 7083.
[11] N.H. Pilkington, R. Robson, Aust. J. Chem. 23 (1970) 2225.
[12] (a) H. Okawa, S. Kida, Bull. Chem. Soc. Jpn. 16 (1972) 1759;
(b) H. Sakiyama, K.I. Motoda, H. Okawa, S. Kida, Chem. Lett. (1991) 1133;
(c) Y. Miyazato, M. Ohba, H. Okawa, Bull. Chem. Soc. Jpn. 78 (2005) 1646.
[13] R.R. Gagne, C.L. Spiro, T.J. Smith, C.A. Hamann, W.R. Thies, A.K. Shiemeke, J. Am. Chem. Soc. 103 (1981) 4073.
[14] S.S. Tandon, L.K. Thompson, J.N. Bridson, C. Benelli, Inorg. Chem. 34 (1995) 5507.
[15] K.K. Nanda, S.K. Dutta, S. Baitalik, K. Venkatsubramanian, K. Nag, J. Chem. Soc., Dalton Trans. (1995) 1239.
[16] F.H. Allen, Acta Cryst. B58 (2002) 380.
[17] M. Pascu, M. Andruh, A. Muller, M. Schmidtmann, Polyhedron 23 (2004) 673.
[18] T. Chattopadhyaya, K.S. Banu, A. Banerjee, J. Ribas, A. Majee, M. Nethaji, D. Das, J. Mol. Struct. 833 (2007) 13.
[19] A.B.P. Lever, Inorganic Electronic Spectroscopy, Elsevier, Amsterdam, The Netherlands, 1984, p 553–556.
[20] Separation of the products, characterization and their chemical behaviors are under investigation and that work will be published elsewhere.
[21] Z. Otwinowski, W. Minor, in: C.W. Carter Jr., R.M. Sweet (Eds.), Processing of X-ray Diffraction Data Collected in Oscillation Mode, Methods in Enzymology, vol. 276: Macromolecular Crystallography, Academic Press, New York, 1997, part A, pp. 307–326.
[22] SHELX97 Programs for Crystal Structure Analysis (Release 97-2). G.M. Sheldrick, University of Göttingen, Germany, 1998.
[23] L.J. Farrugia, J. Appl. Crystallogr. 32 (1999) 837.